

# Implementation of the DE-LEACH Protocol in LoRa Communication Systems to Enhance WSN Lifetime

Angelina Tri Wahyuni<sup>1</sup>, Yoyok Heru Prasetyo Isnomo<sup>2\*</sup>, M. Nanak Zakaria<sup>3</sup>

<sup>1,2,3</sup> Digital Telecommunication Network Study Program, Department of Electrical Engineering, State Polytechnic of Malang, 65141, Indonesia

<sup>1</sup>[2141160070@student.polinema.ac.id](mailto:2141160070@student.polinema.ac.id), <sup>2</sup>[yoyok.heru@polinema.ac.id](mailto:yoyok.heru@polinema.ac.id), <sup>3</sup>[nanakzach@polinema.ac.id](mailto:nanakzach@polinema.ac.id)

**Abstract**—Energy efficiency is a major challenge in Wireless Sensor Networks (WSN) due to power limitations on sensor nodes. This study implements the Distance and Energy-aware LEACH (DE-LEACH) protocol in the LoRa communication system to increase network lifetime. The evaluation was conducted through simulation with 16 nodes and hardware testing based on ESP32, LoRa RA-02 module, DHT11 sensor, MQ-2, voltage sensor, and ACS712. Simulation results show that DE-LEACH extends network lifetime to  $\pm 2800$  rounds, with First Node Dead (FND) at round 1900, Last Node Dead (LND) at round 2900, and cumulative energy consumption of 16J. Compared to REACT-LEACH, DE-LEACH delays FND by  $\pm 1300$  rounds longer. In hardware implementation, the DE-LEACH system lasted up to  $\pm 289$  rounds, longer than the non-clustering method ( $\pm 303$  rounds vs.  $\pm 245$  active node rounds), with an average energy consumption per round that was 12–18% lower. The integration of LoRa in the SF7, BW125 kHz, and CR 4/5 configuration enables low-power long-range communication without degrading the Packet Delivery Ratio (PDR). These findings confirm that DE-LEACH is capable of distributing the energy load more evenly, improving power consumption efficiency, and significantly extending the lifetime of WSNs, both at the simulation level and in real-world implementations.

**Keywords**—DE-LEACH, Energy Efficiency, LoRa, Network Lifetime, Wireless Sensor Network.

## I. INTRODUCTION

Wireless Sensor Networks (WSNs) consist of a large number of spatially distributed sensor nodes designed to cooperatively monitor physical or environmental parameters such as temperature, humidity, pressure, and gas concentration. These networks play a crucial role in various applications, including environmental monitoring, smart agriculture, industrial automation, and Internet of Things (IoT) systems. Despite their widespread adoption, the limited energy capacity of sensor nodes remains a fundamental constraint that directly impacts network longevity, reliability, and maintenance cost [1], [2].

Energy efficiency in WSNs is strongly influenced by the routing protocol, particularly in large-scale deployments where direct communication between sensor nodes and the sink leads to excessive energy consumption. Clustering-based routing protocols have therefore been widely adopted to reduce transmission distance and balance energy usage among nodes [3]. Among these protocols, the Low Energy Adaptive Clustering Hierarchy (LEACH) is one of the earliest and most widely referenced solutions due to its distributed clustering mechanism and data aggregation capability [4], [5]. LEACH periodically rotates the role of Cluster Head (CH) among nodes to distribute energy consumption more evenly across the network.

However, conventional LEACH suffers from several limitations. The random selection of CHs does not consider residual energy or the distance between nodes and the sink, which can result in premature node failures and uneven energy depletion [6], [7]. To address these shortcomings, several enhanced variants of LEACH have been proposed. One notable

improvement is the Distance and Energy-Aware LEACH (DE-LEACH) protocol, which integrates residual energy and distance metrics into the CH selection process, thereby improving network stability and prolonging network lifetime [8], [9]. Recent studies have demonstrated that DE-LEACH outperforms traditional LEACH and other variants in terms of energy efficiency, First Node Dead (FND), and Last Node Dead (LND) metrics [10], [11].

In parallel with routing protocol development, Low Power Wide Area Network (LPWAN) technologies have emerged as a promising communication solution for large-scale WSN deployments. Among these technologies, Long Range (LoRa) communication has gained significant attention due to its long transmission range, low power consumption, and robustness in harsh environments [12], [13]. LoRa employs Chirp Spread Spectrum (CSS) modulation and allows flexible configuration of Spreading Factor (SF), Bandwidth (BW), and Coding Rate (CR), enabling a trade-off between data rate, energy consumption, and communication reliability [14], [15].

Although numerous studies have explored LEACH-based routing protocols and LoRa-based communication systems independently, research that integrates DE-LEACH with LoRa communication in a real WSN environment remains limited. Most existing LoRa-related works primarily focus on coverage analysis, signal propagation, or throughput performance without incorporating adaptive clustering mechanisms that consider energy and distance metrics [16], [17]. Furthermore, many studies rely solely on simulation-based evaluations, lacking validation through real hardware implementation. This creates a research gap in understanding the practical

\*Corresponding author

performance of DE-LEACH when deployed in LoRa-based WSN systems under realistic operating conditions [18], [19].

To address this gap, this study presents the implementation and performance evaluation of the DE-LEACH protocol in a LoRa-based WSN communication system through both simulation and real hardware deployment. The contributions of this research are threefold. First, it provides a comprehensive comparison of DE-LEACH with REACT-LEACH and non-clustering approaches using key performance indicators, including network lifetime, cumulative energy consumption, number of active nodes, and throughput. Second, it evaluates network longevity using FND and LND metrics in both simulated and real environments. Third, it demonstrates how optimized LoRa parameter configurations (SF, BW, and CR) can support energy-efficient clustering while maintaining reliable long-distance communication. The results of this study are expected to contribute to the development of sustainable and scalable WSN solutions for future IoT applications.

## II. METHOD

Research on lifetime optimization in Wireless Sensor Networks (WSN) has been extensively conducted through the development of various LEACH protocol variants [10]. One of these is REACT-LEACH, which takes residual energy into account in the selection of Cluster Heads (CH), but its energy load distribution is still uneven, resulting in suboptimal network performance [11]. On the other hand, a number of studies have attempted to integrate LoRa technology with clustering algorithms, but most of them focus on coverage and data transmission reliability. The aspect of energy efficiency, especially in the context of distance- and energy-based adaptive CH selection, is still rarely discussed in depth [12], [13]. Furthermore, research implementing the integration of DE-LEACH with LoRa on real hardware with sensor-based energy measurements is still very limited. Based on these gaps, this study focuses on testing the performance of the DE-LEACH protocol on LoRa-based WSN, both through simulation and real implementation, as well as conducting a direct comparison with REACT-LEACH and non-clustering methods using the same evaluation parameters.

### A. System Architecture

The system architecture in this study implements the DE-LEACH protocol with a centralized Cluster Head (CH) selection mechanism. Each node sends residual energy and position information to the sink, then the sink calculates the CH selection probability based on distance and remaining energy parameters.

The CH selection results are announced back to all nodes so that cluster formation takes place in a coordinated manner [14]. In this architecture, there are three main entities, namely sensor nodes, CH, and sinks. The sensor nodes are built using ESP32 connected to DHT11 (temperature and humidity), MQ-2 (gas), ACS712 (current), voltage sensors, and LoRa RA-02 communication modules.

Member nodes send data to the CH, which then aggregates the data before forwarding the information to the sink. The sink

acts as a control center and data storage, enabling the entire system to run in a structured and energy-efficient manner.

### B. Simulation and Implementation

In the simulation stage, the network consists of 16 nodes randomly placed in an area measuring  $100 \times 100$  meters with the sink located at the center. Node distribution is set using different random seeds in each experiment to ensure representative scenario variation.

Each configuration was tested at least 10 times, and the results were averaged and presented with a 95% confidence interval to obtain statistical validity. Furthermore, hardware implementation was carried out using ESP32-DevKitC equipped with a LoRa RA-02 module at a frequency of 433 MHz with transmission parameters of TX power 8 dBm, Spreading Factor (SF) 7, Bandwidth (BW) 125 kHz, and Coding Rate (CR) 4/5. The system's power source comes from a 2200 mAh Li-Ion 18650 battery.

### A. Setup Phase

The set-up phase begins with initialization on the sensor and sink nodes. Each node first sends its identity (ID), position, and residual energy *information* to the sink. This data is used by the sink to determine the Cluster Head (CH) based on the probability equation in the DE-LEACH algorithm, which considers distance and residual energy factors [15].

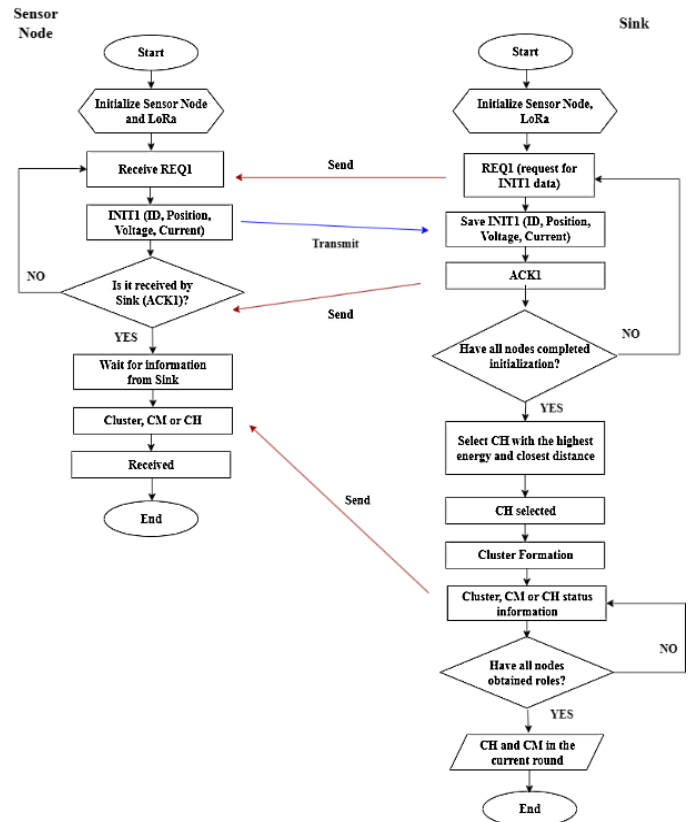


Figure 1. Setup phase flowchart

After the selection is complete, the sink announces the node selected as the CH, then the other nodes automatically select

the nearest CH to form a cluster. To ensure orderly communication, the sink compiles a TDMA (Time Division Multiple Access) transmission schedule, equipped with a guard time of 10 ms on each slot.

This mechanism ensures that there are no collisions between transmissions, thereby maintaining energy efficiency and communication reliability within the network [16].

### C. Steady State Phase

In the steady-state phase, each member node transmits sensor data to the Cluster Head (CH) according to a predetermined schedule in TDMA slots. This mechanism prevents data collisions because each node takes turns transmitting. After receiving data from all members, the CH performs an aggregation process to reduce redundancy, then forwards the compressed data to the sink. Meanwhile, nodes that are not transmitting are switched to sleep mode to reduce energy consumption [17]. In this way, energy usage becomes more efficient, communication load distribution is more evenly distributed, and network life can be extended.

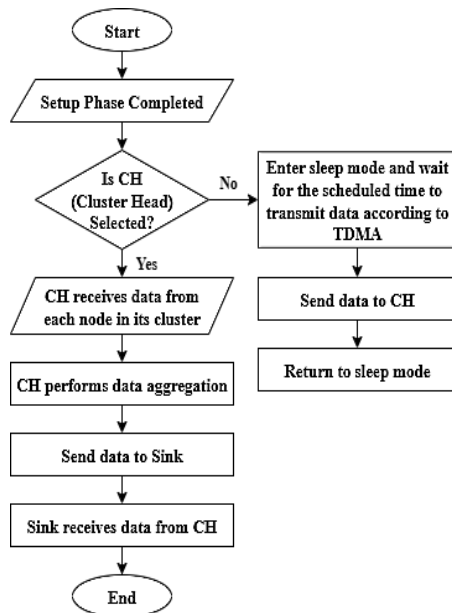


Figure 2. Steady state flowchart

### D. Energy Measurement

Energy measurement is performed using voltage and current sensors (ACS712). Energy is calculated using:

$$E = V \cdot I$$

Sampling was performed at a frequency of 100 Hz, with an integration window per round. The data was corrected with zero calibration (baseline subtraction). Energy consumption was divided into four categories: transmit (TX), receive (RX), idle, and sleep, so that it could be fairly compared with the simulation model. The ESP32 ADC has a resolution of 12 bits. In this study, it was configured in 11-bit effective resolution mode to balance sampling speed and reading stability.

### E. DE-LEACH Protocol

The DE-LEACH topology consists of several clusters with one Cluster Head (CH) in each cluster. Sensor nodes are marked with small circles, while CHs are marked with large blue circles. CHs function as communication centers in clusters, receiving data from member nodes and then sending aggregated data to sinks or base stations. Sinks act as control centers and receive data from all clusters [18].

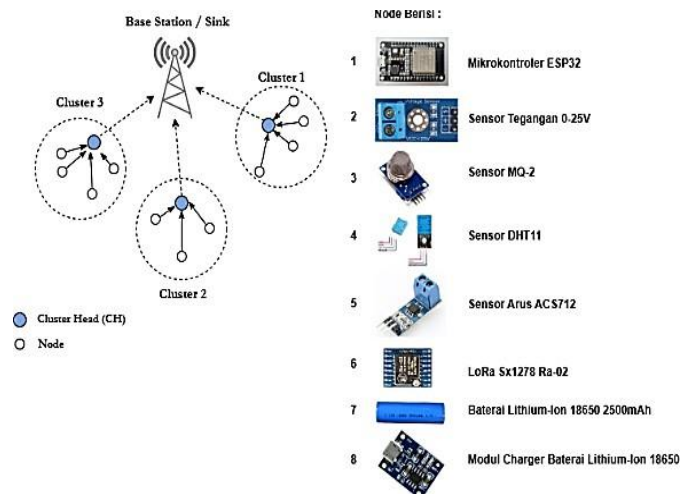


Figure 3. DE-LEACH protocol

The hardware that makes up each node is shown on the right side of the image, consisting of: ESP32 as the main microcontroller, voltage sensor, MQ-2 sensor, DHT11 sensor, ACS712 current sensor, LoRa RA-02 module, 18650 Li-Ion battery, and battery charger module. This combination of devices allows the node to monitor the environment while supporting long-distance communication with low energy consumption.

## III. RESULTS AND DISCUSSION

### A. Result of System Implementation

This section discusses hardware design. Figure 4 shows the assembled device.

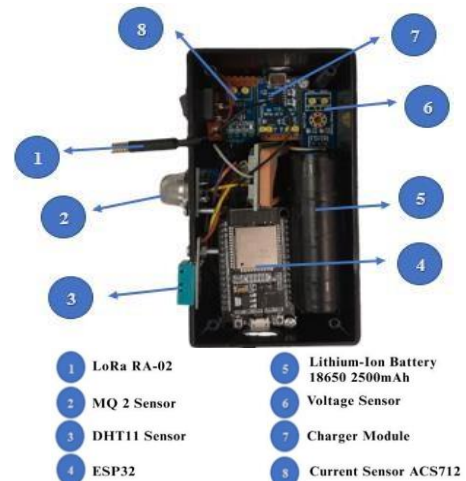


Figure 4. Device result

### B. Results of Node and Sink Deployment Plotting

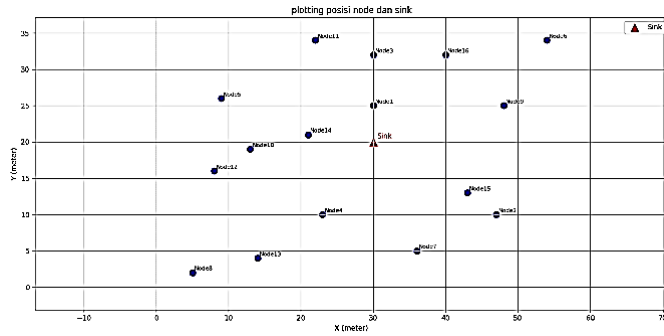


Figure 5. Node and sink distribution plot

The plot shows the distribution of 16 sensor nodes and one sink on a 2D coordinate field (X, Y in meters). Nodes are represented as blue circles labeled node1 to node16, while the sink is depicted as a red triangle at the center of the network area. The sink acts as a data collection center, both directly from the nodes and through the Cluster Head (CH). Placing the sink at the center point is strategic as it minimizes the average communication distance with the nodes, thereby reducing overall energy consumption.



Figure 6. Illustration of cluster formation and CH allocation

The illustration shows the formation of clusters and the allocation of Cluster Head (CH) and Cluster Member (CM) roles in the DE-LEACH network. The sink is marked in blue central data receiver, while the colored nodes indicate the cluster divisions.

- Cluster 1 (Red): CH = Node 1; CM = Node 3, 6, 11
- Cluster 2 (Yellow): CH = Node 2; CM = Node 7, 9
- Cluster 3 (Green): CH = Node 4; CM = Node 5, 8, 10

The placement of CHs is distributed evenly across the network, which minimizes the communication distance between CMs and their respective CHs. This configuration reduces the transmission energy required for intra-cluster communication. Each CH then aggregates the collected data before forwarding it to the sink. Such a mechanism not only balances the communication load among nodes but also

prevents rapid energy depletion in specific nodes, thereby extending the overall network lifetime Simulation of DE-LEACH in Spyder.

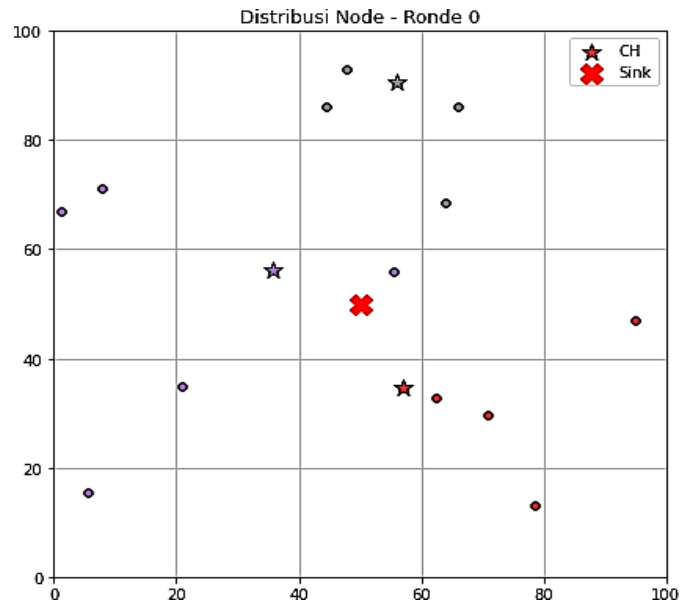


Figure 7. Node Distribution Round 0

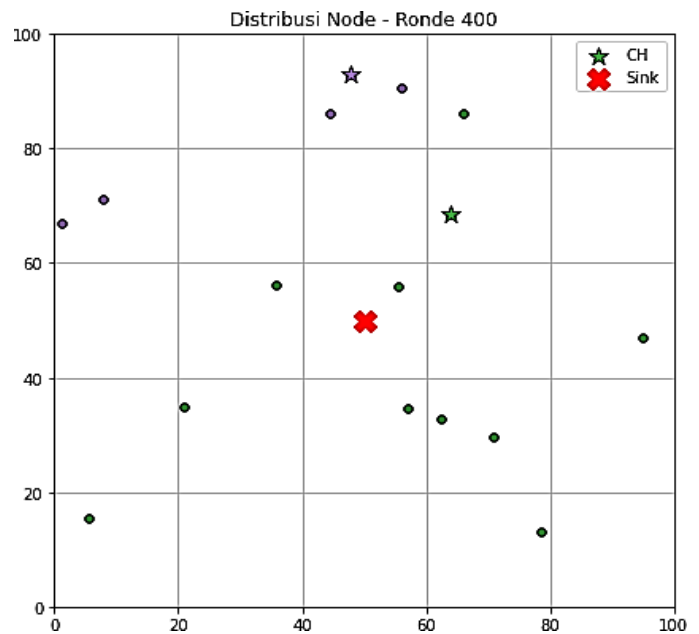


Figure 8. Distribution of nodes at round 400

At round 400, the energy of several nodes begins to decrease, indicated by the change in color to darker shades. This reflects the effectiveness of DE-LEACH in balancing energy consumption, although communication activities still cause energy depletion. Most nodes in the upper area are still active because of their position near the CH, making energy consumption more efficient. The selected CHs are spread across regions with still-alive nodes.

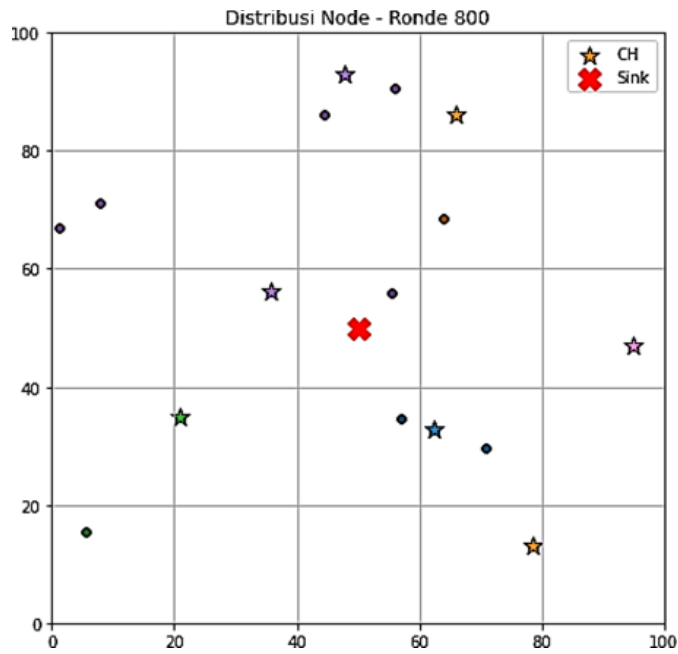


Figure 9. Node distribution round 800

At round 800, the energy drop becomes more significant indicated by the darker color of the nodes. DE-LEACH is still able to select CH adaptively based on remaining energy and distance to the sink, but an imbalance in cluster distribution begins to emerge due to the decreasing number of active nodes in certain areas of the network.

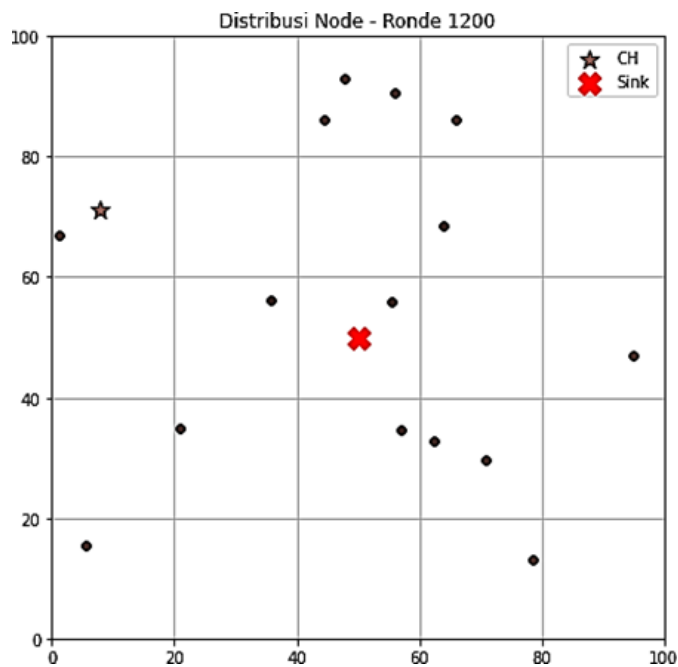


Figure 10. Distribution of nodes at round 1200

In round 1200, the number of active nodes continues to decline and only one cluster is formed. The nodes that are still alive are marked with dark circles indicating very low energy condition. The increasingly dull color indicates critical battery

status. Only one Cluster Head (CH) meets the DE-LEACH criteria, but this CH has a heavier workload because it has to accommodate data from distant nodes.

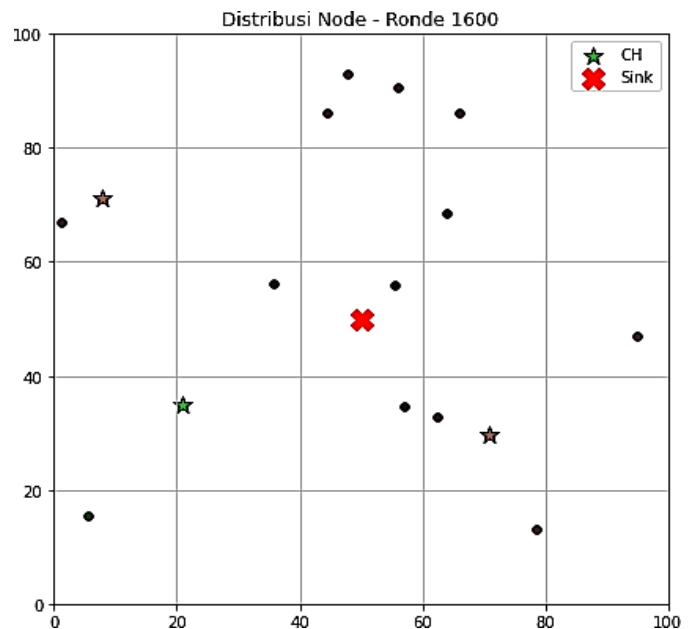


Figure 11. Distribution of round node 1600

In round 1600, the network enters the final phase of its life cycle with most nodes in a critical energy condition. The number of Cluster Heads (CH) is no longer optimal and the distribution of clusters is less balanced. However, DE-LEACH still effectively maintains CH selection efficiency even as resources are nearly depleted.

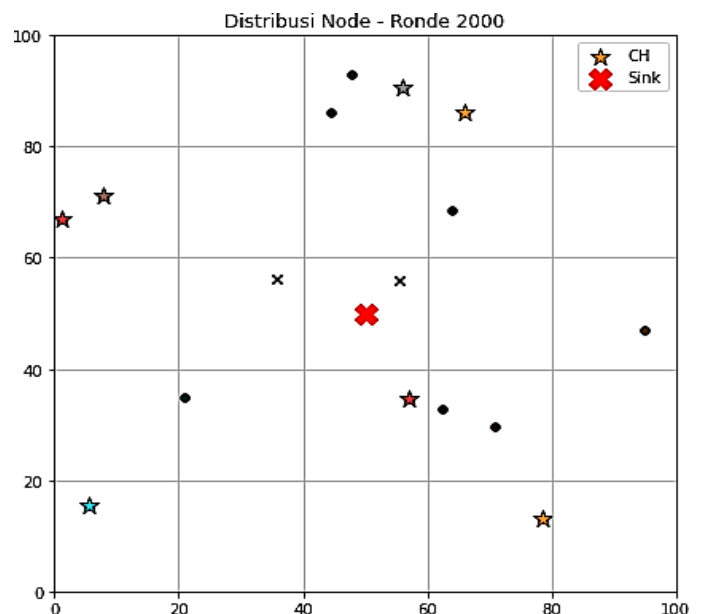


Figure 12. Distribution of nodes in round 2000



In round 2000, several nodes are dead marked with a black cross symbol due to energy depletion. The clusters formed have become less efficient because the distance from the Cluster Head (CH) to the Cluster Manager (CM) is either too far or too close between CHs. This condition accelerates the energy consumption of the nodes and decreases the performance of the network, although DE-LEACH is still able to maintain operation until this round.

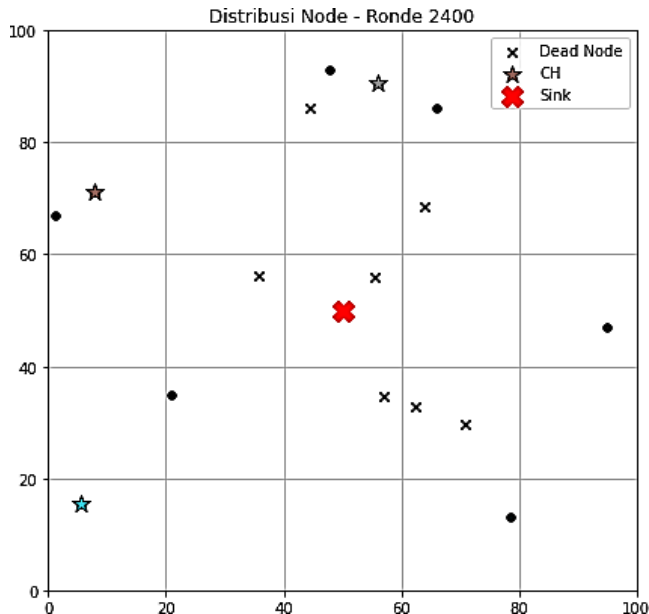


Figure 13. Distribution of nodes at round 2400

In round 2400, the number of dead nodes increases significantly, leading to a sharp decline in active nodes. The position of the Cluster Head (CH) becomes less ideal as the remaining nodes are unevenly distributed, causing a decrease in communication efficiency and data aggregation. The remaining energy is depleted mainly for transmission and maintaining the continuity of nodes in the network.

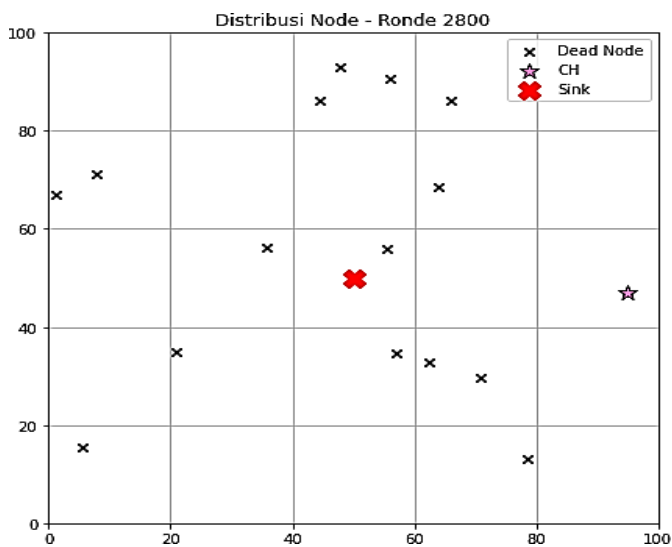


Figure 14. Distribution of round 2800 nodes

In round 2800, the network enters the final operational phase with most nodes having died due to energy depletion. Only one node remains active and is selected as the Cluster Head (CH), located at the right edge of the network area. This situation indicates that although DE-LEACH has successfully extended the network's lifespan, there are still limitations when all the node's energy eventually runs out.

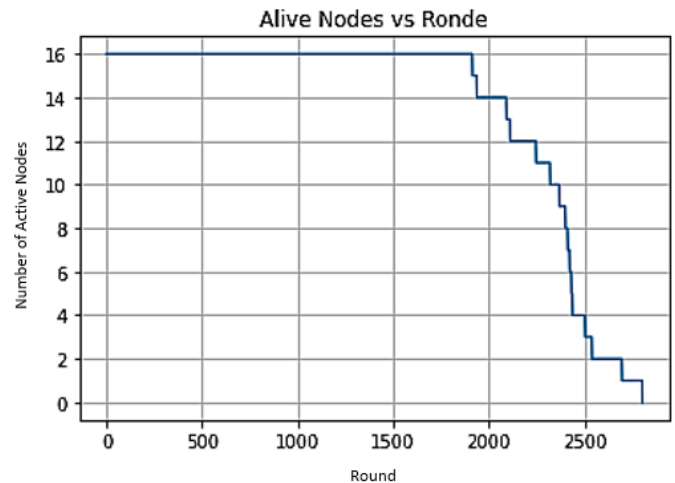


Figure 15. Alive nodes vs rounds

The graph shows the number of active nodes throughout the simulation. From round 0 to around 1900, all 16 nodes remain active because the energy is still sufficient and the CH selection is optimal. Entering rounds 1900–2500, the number of nodes begins to decrease significantly due to some nodes running out of energy, especially those that frequently become CH or are far from the sink. After round 2500, the number of active nodes continues to decrease rapidly until all nodes are dead around round 2900, marking the end of the networks.

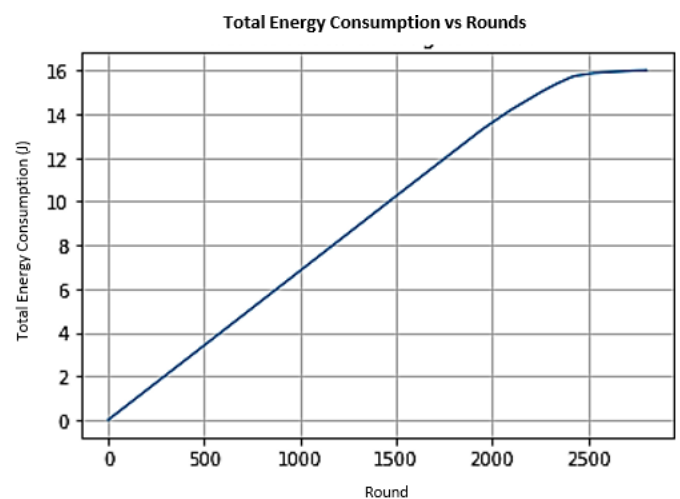


Figure 16. Total energy consumption vs rounds

The graph shows an increase in total energy consumption as the communication rounds increase. In rounds 0–500, energy rises sharply to about 2.85 J due to the initialization process involving all nodes in selecting the CH and sending initial data. In rounds 500–1500, the rate of increase slows from 3.8 J to 9.5 J, indicating that the system enters a stable phase with a more even distribution of energy thanks to the DE-LEACH algorithm. After round 1500, energy consumption increases more gradually until it reaches 16 J at round 2800, influenced by the decrease in the number of active nodes as some have already died.

### C. Comparison of Live Nodes on DE-LEACH and REACT-LEACH Protocols in Spyder

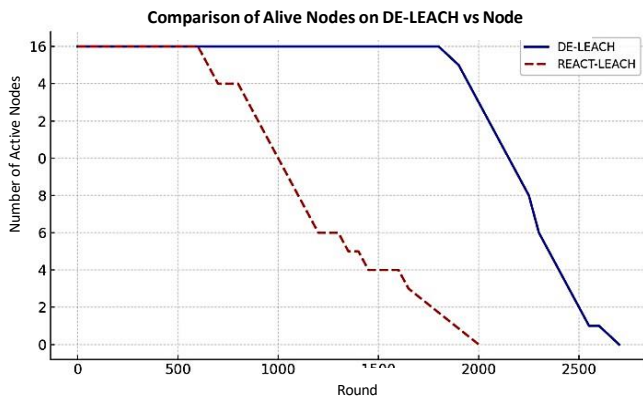


Figure 17. Comparison of live nodes on DE-LEACH and REACT-LEACH protocols

The DE-LEACH protocol demonstrates superior energy efficiency when compared to REACT-LEACH, primarily due to its refined cluster head (CH) election strategy. In simulation evaluations, the network employing DE-LEACH maintains full node participation—meaning all sensor nodes remain operational—until approximately round 1900. By contrast, under REACT-LEACH, the first node depletes its energy as early as round 600. This stark difference arises from DE-LEACH's dual-criteria CH selection mechanism, which jointly evaluates the residual energy of each candidate node and its Euclidean distance to the sink. This approach ensures that only nodes with sufficient energy reserves and favorable topological positions are elected as cluster heads, thereby distributing the communication and computational burden more evenly across the network.

Conversely, REACT-LEACH employs a less dynamic CH selection process that does not sufficiently prioritize current energy levels during the election phase. As a result, low-energy nodes may be inadvertently selected as cluster heads, causing them to exhaust their batteries prematurely due to the high energy cost of data aggregation and long-haul transmission. This imbalance accelerates energy depletion in critical regions of the network, ultimately triggering cascading node failures. While the REACT-LEACH-based network collapses entirely

by round 2000, DE-LEACH continues to sustain communication with a significant portion of its nodes active until round 2700. This extended operational window underscores DE-LEACH's effectiveness in prolonging network lifetime through an intelligent, context-aware clustering mechanism that harmonizes energy awareness with spatial topology. Consequently, DE-LEACH not only delays the first node death (FND) but also maximizes the last node death (LND), making it particularly suitable for long-duration WSN deployments where maintenance and battery replacement are impractical.

### D. Results of Device Testing

#### 1) Non-Clustering Data

	Round	NodeID	X	Y	Voltage	Current	InitTime	dataTime	idleTime	Temperature	Humidity	Gas
1	1	1	30	25	3.19	615.36	300	400	24900	26.7	64	1.81
2	1	2	47	10	4.08	748.1	300	400	24900	25.8	58	6.01
3	1	3	30	32	4.4	784.17	300	400	24900	26.7	58	9.87
4	1	5	9	26	3.69	984.72	300	400	24900	25.8	58	5.18
5	1	6	54	34	4.34	765.65	300	400	24900	27.1	54	4.5
6	1	7	36	5	4.48	810.38	300	400	24900	25.3	57	20.97
7	1	8	5	2	3.69	984.72	300	400	24900	26.7	59	0
8	1	9	48	25	4.58	984.72	300	400	24900	28	54	5.91
9	1	10	13	19	3.86	708.66	300	400	24900	26.6	47	14.37
10	1	12	8	16	3.65	681.01	300	400	24900	24.8	53	0
11	1	13	14	4	3.71	731.75	300	400	24900	27	45	1.03
12	2	1	30	25	3.21	614.16	300	400	24900	26.7	64	1.91
13	2	2	47	10	4.09	747.14	300	400	24900	25.8	58	5.96
14	2	3	30	32	4.37	781.04	300	400	24900	26.7	57	9.73
15	2	5	9	26	3.68	984.72	300	400	24900	25.8	58	5.33
16	2	6	54	34	4.22	765.65	300	400	24900	27.1	54	4.4
17	2	7	36	5	4.52	811.1	300	400	24900	25.3	57	20.63
18	2	8	5	2	3.69	984.72	300	400	24900	26.7	59	0
19	2	9	48	25	4.56	984.72	300	400	24900	28	54	5.77
20	2	10	13	19	3.84	705.54	300	400	24900	26.5	47	14.61
21	2	12	8	16	3.65	681.01	300	400	24900	24.8	53	0
22	2	13	14	4	3.71	728.38	300	400	24900	27	45	1.32
23	3	1	30	25	3.22	611.75	300	400	24900	26.7	64	2.1
24	3	2	47	10	4.07	743.77	300	400	24900	25.8	58	5.72
25	3	3	30	32	4.38	782.49	300	400	24900	26.7	57	9.73

Figure 18. Non-clustering excel display results

Testing of the non-clustering communication system was conducted with each node sending data directly to the sink without going through a CH. The test result table displays data for each round, including Node ID, position (X, Y), and energy parameters (Voltage 3.19–4.58 V and Current 600–984 mA). The communication time pattern consists of initTime 300 ms, dataTime 400 ms, and idleTime 24.9 seconds, which indicates a periodic working mechanism with sleep mode for energy efficiency. Sensor data includes temperature (25–28°C), humidity (47–64%), and gas (0.97–20.57). The results show that each node consistently sends data according to the schedule, although the non-clustering method has the potential to create uneven energy consumption among nodes.

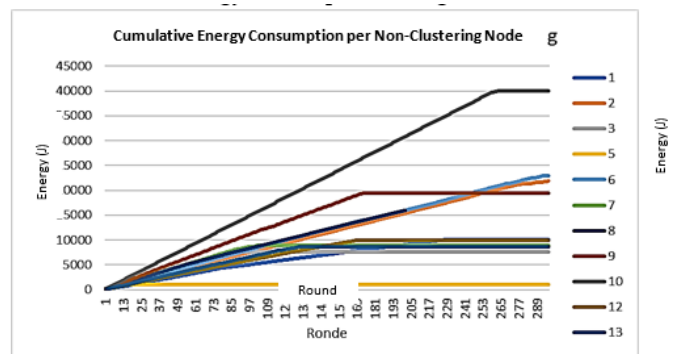


Figure 19. Cumulative energy consumption graph per non-clustering node

The graph above shows the cumulative energy consumption of each node against the number of communication rounds. In this model, each round consists of the INIT phase, which includes sensor activation, LoRa, and initial synchronization; and the Data Transmission phase as the main phase with the highest energy consumption due to the data transmission process to the sink using LoRa. The results indicate that direct communication without clustering leads to high energy requirements for each node. The transmission energy  $E_{tx}$  can be calculated using formula (1)

$$E_{tx} = P_{tx} \times t_{tx} \quad (1)$$

where:

$P_{tx}$  = power used during transmission (in watts)

$t_{tx}$  = duration of transmission (in seconds)

During the Idle/Sleep phase, nodes switch to power-saving mode after data transmission until the next round. Energy consumption during this phase is relatively small, but it still accumulates in the total energy calculation of the network. Thus, the cumulative energy consumption per round is the sum of the INIT phase, data transmission, and idle/sleep. Therefore, the cumulative energy of a node in the  $r$ -th round can be calculated using the formula:

$$\text{Cumulative energy} = (V \times I) / 1000 \times (\text{initTime} + \text{dataTime} + \text{idleTime}) \quad (2)$$

where:

$E$  = Energy (Joule)

$V$  = Voltage (V)

$I$  = Current (mA)

$t$  = Total active time in seconds (the sum of initTime, dataTime, and idleTime, converted to seconds)

The graph shows a trend of increasing energy consumption until the node reaches a critical point, which is when the energy drops below the minimum operational voltage and the node is considered dead. This pattern is important for evaluating the efficiency of communication systems, where a slower rate of increase in cumulative energy indicates more economical consumption and a longer network lifespan.

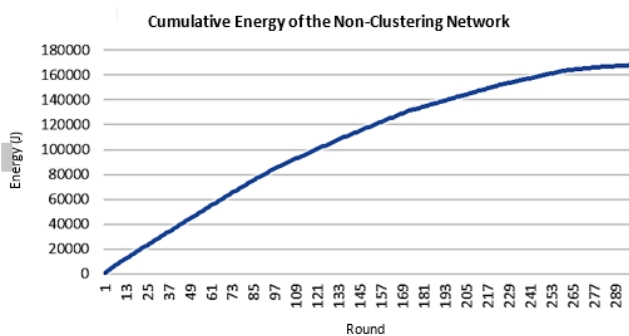


Figure 20. Cumulative energy graph of the non-clustering network

The cumulative energy consumption curve provides critical insight into the temporal energy dynamics of the wireless sensor network (WSN) under a non-clustering communication architecture. During the initial operational phase (rounds 1–100), the network exhibits a steep rise in total energy expenditure, reflecting the fact that all sensor nodes are simultaneously active and engaged in continuous sensing, local processing, and direct transmission to the sink. This phase is characterized by high broadcast redundancy and lack of data aggregation, which inherently amplifies energy overhead. As the simulation progresses into the intermediate phase (rounds 100–200), the slope of the energy curve begins to moderate. This deceleration is not due to improved efficiency, but rather to the progressive failure of nodes—particularly those located farther from the sink or burdened with disproportionate communication loads—whose batteries deplete rapidly in the absence of load-balancing mechanisms. By the final phase (rounds 200–300), the curve plateaus significantly, indicating that a large fraction of the network has become non-functional, with only a sparse subset of nodes remaining operational. At round 303, the cumulative energy consumption stabilizes at approximately 170,000 joules, not because energy is conserved, but because the majority of nodes have already exhausted their power reserves.

This pattern reveals fundamental limitations of non-clustering topologies in WSNs: without hierarchical organization or intelligent traffic coordination, energy dissipation becomes highly unbalanced. Nodes closest to the sink or those with initially higher energy may be overutilized, while others suffer from inefficient long-range transmissions. Consequently, the network experiences premature partitioning, severely truncated operational lifetime, and eventual total collapse once the last functional node depletes its energy. These findings underscore the critical need for energy-aware clustering strategies—such as those employed in DE-LEACH—to mitigate hotspot formation, extend network longevity, and ensure sustainable data delivery over extended deployment periods.

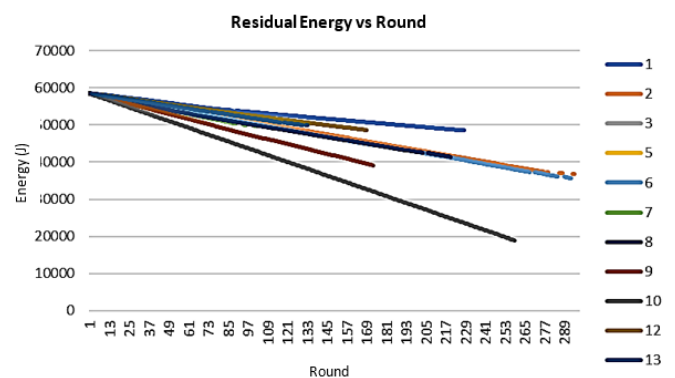


Figure 21. Residual energy vs round

The graph of residual energy per node shows a gradual decrease in energy on the non-clustering system, where each node sends data directly to the sink without intermediaries. All



nodes start with an energy of  $\pm 58.608$  J (based on the calculation of a battery capacity of  $2 \times 2200$  mAh). The pattern of energy decrease is linear, indicating that energy consumption per round is relatively constant due to the absence of a clustering mechanism. Variations among nodes are clearly visible, for example, Node 3 runs out of energy around the 290th round at a consumption rate of  $\pm 202$  J/round, while Node 12 and 13 are more efficient with a consumption of  $\pm 34$ – $36$  J/round and still have about  $\pm 48,000$  J remaining by the 300th round. This difference is influenced by the distance of nodes to the sink, where nodes that are farther away require greater transmission energy.

#### E. Clustering DE-LEACH Data

1	Round	Cluster	CH_ID	Node_ID	Tegangan	Arus	Temperatur	Kelembaban	Gas
2	1	1	13	4	3.96	722.88	29.5	52	15.02
3	1	1	13	7	3.69	744.53	28.4	64	8.75
4	1	1	13	8	3.63	762.54	28.7	57	24.41
5	1	1	13	10	3.96	737.75	28.9	59	24.53
6	1	1	13	13	3.61	697.98	25.3	73	17.68
7	1	2	9	2	4.17	806.66	26.8	74	18.79
8	1	2	9	9	4.12	740.17	25.2	49	19.96
9	1	3	11	1	3.82	825.19	26.7	72	10.27
10	1	3	11	3	4.04	722.54	27.3	68	10.46
11	1	3	11	5	3.69	729.9	26.2	45	16.36
12	1	3	11	11	4.02	763.53	26.4	46	23.51
13	2	1	2	2	4.16	798.8	27.4	72	19.19
14	2	1	2	7	3.68	733.21	28.2	65	8.77
15	2	1	2	9	4.12	767.04	25	48	19.85
16	2	2	8	4	3.96	729.61	29.5	55	14.88
17	2	2	8	8	3.63	757.34	28.4	56	23.47
18	2	2	8	13	3.61	713.37	25.8	72	16.64
19	2	3	11	1	3.82	833.61	26.7	71	9.42
20	2	3	11	3	4.03	718.8	27.7	68	10.8
21	2	3	11	5	3.68	721.83	26.7	45	16.27
22	2	3	11	10	3.95	746.13	29	57	23.47
23	2	3	11	11	4.01	763.88	26.1	46	22.38
24	3	1	1	1	3.81	822.29	27.1	73	9.35
25	3	1	1	3	4.03	719	27.4	69	10.7
26	3	1	1	4	3.95	719.24	29.8	55	15.72

Figure 22. Excel clustering output

Testing of LoRa-based communication systems using the clustering method with the DE-LEACH protocol was conducted to evaluate energy efficiency. Nodes are grouped into clusters with one cluster head (CH) selected based on residual energy and distance to the sink. Member nodes (CM) only send data to the CH, while the CH performs aggregation and sends the results to the sink. Measurement results show a voltage variation between 3.61–4.32 V and current between 697.98–833.61 mA, where higher energy consumption occurs during transmission or sensor processing. Environmental sensor data is relatively stable, with temperatures ranging from 25.2–29.8°C, humidity from 45–73%, and gas levels from 8.75–54.53. Nodes acting as CH consume more energy because they receive data from the cluster members and send it to the sink simultaneously. Variations in voltage, current, and sensor values reflect the dynamics of the workload and environmental conditions in each communication round.

This elevated energy demand on CHs validates the importance of DE-LEACH's rotation mechanism, which prevents any single node from being overburdened across consecutive rounds. Furthermore, the observed current spikes align closely with LoRa transmission events under Spreading Factor 7 and 125 kHz bandwidth, confirming that PHY-layer configuration directly influences power draw. The stability of environmental readings also suggests that the system maintains

reliable sensing fidelity despite dynamic energy fluctuations, reinforcing the robustness of the integrated DE-LEACH–LoRa architecture in real-world deployment scenarios.

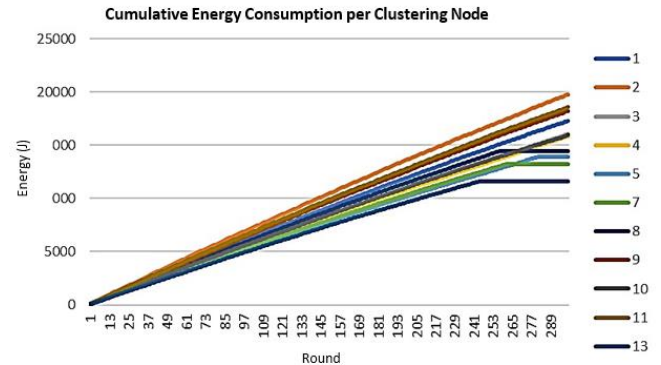


Figure 23. Cumulative energy consumption graph per clustering node

The cumulative energy consumption graph per node in the clustering scheme shows relatively constant energy usage over 300 rounds without significant spikes. In round 289, Node 2 and Node 9 were recorded as the highest energy users, at approximately 20,500 J and 20,300 J respectively, while Node 1 was the lowest with 15,000 J, followed by Node 5 with around 15,200 J. Other nodes ranged from 16,000 to 18,500 J, indicating moderate energy consumption variation. This difference is influenced by the role of nodes in the network, where the clustering mechanism proves to be more efficient as not all nodes need to communicate directly with the sink.

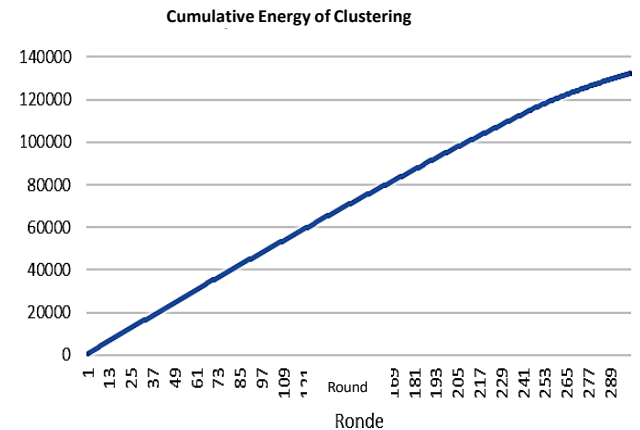


Figure 24. Cumulative energy graph of clustering network

Figure 24 shows the cumulative energy graph of the clustering network with a consistent increase in energy consumption from round 1 to round 289. The nearly linear increase pattern indicates that energy consumption per round is relatively constant due to the clustering mechanism, where CH aggregates and sends data to the sink, while CM only transmits short distances to CH. Towards the end of the simulation, the total cumulative energy reached around 130,000–140,000 J, confirming that clustering can maintain stable energy consumption until the end of the communication period.

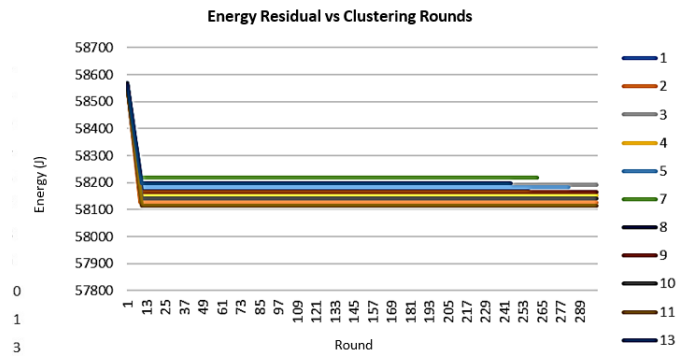


Figure 25. Energy residual vs clustering rounds

The Energy Residual vs Clustering Rounds graph shows that at the beginning of the simulation (Rounds 1–13) there was a significant decrease in energy due to the clustering process and the selection of CH, for example, Node 1 and Node 13 lost about 370–390J. After round 25, energy consumption stabilized with a decrease of only 10–20J over hundreds of rounds, indicating the efficiency of energy distribution through the clustering mechanism. The average initial energy of the nodes was around 58,550J and after stabilizing, it remained around 58,200J, with a total decrease of  $\pm 0.6\%$  from the initial energy

TABEL I.  
COMPARISON OF NON-CLUSTERING AND CLUSTERING DE- LEACH

Comparison	Non-Clustering	Clustering DE-LEACH
Total Cumulative Network Energy	176,000 Joules (289 rounds)	136,000 Joules (289 rounds)
Average Energy Consumption per Round	609 Joules/round	471 Joules/round
Energy Load Distribution	Uneven, nodes located farther from the sink or transmitting data frequently bear higher loads	Even, the load is shared among cluster members with rotating CH (Cluster Head) roles.
Energy Difference Between Nodes	High; residual energy difference between nodes reaches > 25,000 J at the end of simulation	Low; residual energy difference between nodes is only around 100–200 J
Network Lifetime Effectiveness	Shorter lifetime as several nodes deplete the energy much faster	Longer lifetime as all nodes retain energy for a longer duration
Energy Utilization Efficiency	Less efficient (imbalanced load)	More efficient (optimal load distribution)

Table 1 above compares the Non-Clustering and Clustering DE-LEACH methods on WSN. The results show that Clustering DE-LEACH is more efficient with a total energy consumption of 136,000 J over 289 rounds (471 J/round), lower than Non-Clustering at 176,000 J (609 J/round). The Non-Clustering method causes uneven load distribution, where nodes close to the sink run out of energy faster with a residual

difference between nodes of >25,000 J. In contrast, Clustering DE-LEACH distributes the load evenly through CH rotation, resulting in an energy difference between nodes of only 100–200 J. This enables Clustering DE-LEACH to save energy, extend network lifespan, and maintain more optimal performance compared to Non-Clustering.

#### IV. CONCLUSION

This research shows that the DE-LEACH protocol is superior in energy efficiency and network resilience compared to both REACT-LEACH and Non-Clustering systems. In REACT-LEACH, the first node died at round 600 and all nodes ceased operation by round 2000, while in DE-LEACH, the first node only died at round 1900, and there were still active nodes up to round 2700. This proves that DE-LEACH can extend the network lifespan by about 35% longer. Compared to Non-Clustering, DE-LEACH's total energy consumption is also lower (136,000J vs 176,000J) with an average energy usage per round of 471J, which is more efficient than Non-Clustering's 609J/round. Additionally, the energy load distribution in DE-LEACH is more uniform, with a residual energy difference between nodes of only 100–200J, which is much more balanced compared to Non-Clustering's 25,000J. The implementation of DE-LEACH using ESP32 hardware and RA-02 LoRa module shows that this algorithm remains stable for hundreds of rounds, despite facing time synchronization challenges that affect communication efficiency.

Based on these results, it is recommended that further research expands the testing scenarios with a larger number of nodes and more complex environmental conditions to thoroughly test the scalability of the protocol. In addition, there is a need for the development of time synchronization mechanisms between nodes so that the TDMA-based communication schedule can run more precisely, minimizing packet collisions, and improving energy efficiency. Moving forward, the development of adaptive DE-LEACH that can adjust to changes in the number of nodes, dead nodes, or changes in position is essential to enhance the flexibility and resilience of the system in real-world applications of LoRa-based wireless sensor networks.

#### REFERENCES

- [1] O. A. Permata, K. Amiroh, and F. Z. Rahmanti, "Energy efficiency to extend wireless sensor network lifetime using LEACH algorithm," *JIKO*, vol. 3, no. 1, pp. 31–35, 2020.
- [2] K. Fallo, W. Wibisono, and K. N. P. Pamungkas, "Grid-based clustering for LEACH performance improvement," *Jurnal Ilmiah Teknologi Sistem Informasi*, vol. 5, no. 34, pp. 152–161, 2020.
- [3] Panchal, L. Singh, and R. K. Singh, "RCH-LEACH: Residual energy-based cluster head selection," in *Proc. ICE3*, 2020, pp. 322–325.
- [4] Hariyadi *et al.*, "Power efficiency of WSN devices based on LEACH," *Techné*, vol. 20, no. 2, pp. 101–112, 2021.
- [5] P. Mishra, S. K. Alaria, and P. Dangi, "Design and

- comparison of LEACH and improved LEACH,” *IJRITCC*, vol. 9, no. 5, pp. 34–39, 2021.
- [6] Rajput and V. B. Kumaravelu, “FCM clustering and FLS-based CH selection,” *J. Ambient Intell. Humaniz. Comput.*, vol. 12, no. 1, pp. 1139–1159, 2021.
- [7] W. Berlianto *et al.*, “Implementation of LEACH in nRF24L01-based WSN,” *J-PTIK UB*, vol. 5, no. 10, pp. 4680–4688, 2021.
- [8] S. Hossan, S. Akter, and P. K. Choudhury, “Distance and energy aware extended LEACH,” *Telematics and Informatics Reports*, vol. 8, 2022.
- [9] S. Hossan and P. K. Choudhury, “DE-SEP routing protocol for heterogeneous WSNs,” *IEEE Access*, vol. 10, pp. 55726–55738, 2022.
- [10] Ridwan, R. Ferdian, and R. Kurnia, “Optimization of LEACH for stability improvement,” *J. RESTI*, vol. 4, no. 1, pp. 192–200, 2020.
- [11] Y. H. Prasetyo, M. Muladi, and H. Elmunsyah, “Systematic literature review of LEACH development,” *Przegląd Elektrotechniczny*, 2024.
- [12] A. Augustin *et al.*, “A study of LoRa: Long range and low power networks,” *Sensors*, vol. 20, no. 3, 2020.
- [13] F. Adelantado *et al.*, “Understanding the limits of LoRaWAN,” *IEEE Commun. Mag.*, vol. 58, no. 3, pp. 34–40, 2020.
- [14] M. Centenaro *et al.*, “Long-range communications in unlicensed bands,” *IEEE Wireless Commun.*, vol. 27, no. 2, pp. 102–109, 2020.
- [15] R. Sanchez-Iborra and M.-D. Cano, “State of the art in LPWAN solutions,” *Sensors*, vol. 20, no. 6, 2020.
- [16] S. Hossan and J. Islam, “Secondary cluster head based SEP,” *IET Communications*, vol. 18, no. 11, pp. 679–688, 2024.
- [17] J. Petäjäjärvi *et al.*, “Performance of LoRaWAN,” *IEEE Access*, vol. 9, pp. 1425–1437, 2021.
- [18] M. Bor *et al.*, “Do LoRa low-power wide-area networks scale?” *MSWiM*, 2021.
- [19] A. Lavric and V. Popa, “Internet of Things and LoRa™ low-power wide-area networks,” *Sensors*, vol. 21, no. 11, 2021.
- [20] M. K. Mishra and A. Kumar, “A review of wireless sensor networks,” *Int. J. Res. Appl. Sci. Eng. Technol.*, vol. 7, no. 4, pp. 1–5, Apr. 2019.
- [21] Chandanse, P. Bharane, S. Anchan, and H. Patil, “Performance analysis of LEACH protocol in wireless sensor networks,” *SSRN Electron. J.*, 2019.